Laser Physics, Vol. 12, No. 8, 2002, pp. 1191–1198.

Supercontinuum Generation in Photonic-Molecule Modes of Microstructure Cobweb Fibers and Photonic-Crystal Fibers with Femtosecond Pulses of Tunable 1.1–1.5-μm Radiation

A. N. Naumov[1,2], A. B. Fedotov[1,2], I. Bugar[3], D. Chorvat, Jr.[3], V. I. Beloglazov[4], S. O. Konorov[1], L. A. Mel'nikov[5], N. B. Skibina[4], D. A. Sidorov-Biryukov[2], E. A. Vlasova[2], V. B. Morozov[1,2], A. V. Shcherbakov[4], D. Chorvat[3], and A. M. Zheltikov[1,2]

[1] *Physics Faculty, M.V. Lomonosov Moscow State University, Vorob'evy gory, Moscow, 119899 Russia*

e-mail: zheltikov@top.phys.msu.su

[2] *International Laser Center, M.V. Lomonosov Moscow State University, Vorob'evy gory, Moscow, 119899 Russia*

[3] *International Laser Center, Ilkovičova 3, Bratislava, 81219 Slovak Republic*

[4] *Technology and Equipment for Glass Structures Institute, pr. Stroitelei, Saratov, 410044 Russia*

[5] *Saratov State University, Astrakhanskaya ul. 83, Saratov, 410026 Russia*

Received March 9, 2002

Abstract—The modes guided in a ring system of cobweb-microstructure-integrated fibers are shown to have much in common with electron wave functions in a two-dimensional polyatomic cyclic molecule. A high degree of light confinement in waveguide modes of such a photonic molecule enhances nonlinear-optical processes, permitting an octave spectral broadening to be achieved for low-energy femtosecond laser pulses. Supercontinuum-generating abilities of photonic-molecule modes of a cobweb microstructure and guided modes of a photonic-crystal fiber are compared.

1. INTRODUCTION

Microstructure (MS) fibers [1–4] have been finding rapidly growing applications in various areas of photonics in the past few years, expanding into a powerful tool of nonlinear optics, optics of ultrashort pulses, and optical metrology. Unique properties of these fibers offer the possibilities of tailoring the dispersion of guided modes by changing the core–cladding geometry [4] and achieving a high confinement degree of light field in the fiber core due to a high refractive-index step between the core and the cladding in such a fiber [5, 6]. A combination of these properties allows the whole catalog of nonlinear-optical processes to be enhanced. Supercontinuum generation with unamplified nano- and subnanojoule femtosecond pulses [7] is one of the most spectacular manifestations of this enhancement and one of the most impressive results achieved with microstructure fibers in recent years. Supercontinuum generation in microstructure fibers has already resulted in revolutionary changes in optical metrology [8–10]. Creation of practical compact components and devices utilizing the ability of microstructure fibers to enhance nonlinear-optical processes is now on the agenda, suggesting new approaches to frequency conversion of laser radiation [11, 12], generation of few-cycle light pulses with controlled parameters [13], high-order optical harmonic generation [14, 15], as well as the creation of broadband sources for spectroscopic applications [16] and systems with a tunable coherence length for optical coherence tomography [17, 18]. One of the promising applications of microstructure fibers may involve the creation of compact optical data storage and data processing devices operating with ultralow-energy ultrashort laser pulses and using, in particular, various modifications of photon echo—the phenomenon observed in the seminal work by S. Hartmann and his coworkers [19].

The design of the core and the cladding in microstructure fibers is crucial for many functions of such fibers in optical physics [4] and biomedical applications [17, 18]. In particular, microstructure fibers with a photonic-crystal cladding provide new regimes of waveguiding due to a high reflectivity of the cladding around the photonic band gap [1] and allow many of the ideas discussed in connection with photonic crystals to be realized. With a special design of the core and the cladding, a microstructure fiber can be made highly birefringent [20, 21]. In this paper, we will present the results of our nonlinear-optical experiments performed with microstructure fibers of two different designs (Figs. 1a, 1b). Microstructure fibers of the first type are standard holey fibers, which have a structure of a two-dimensional photonic crystal with air holes periodically arranged in glass or fused silica and a single miss-

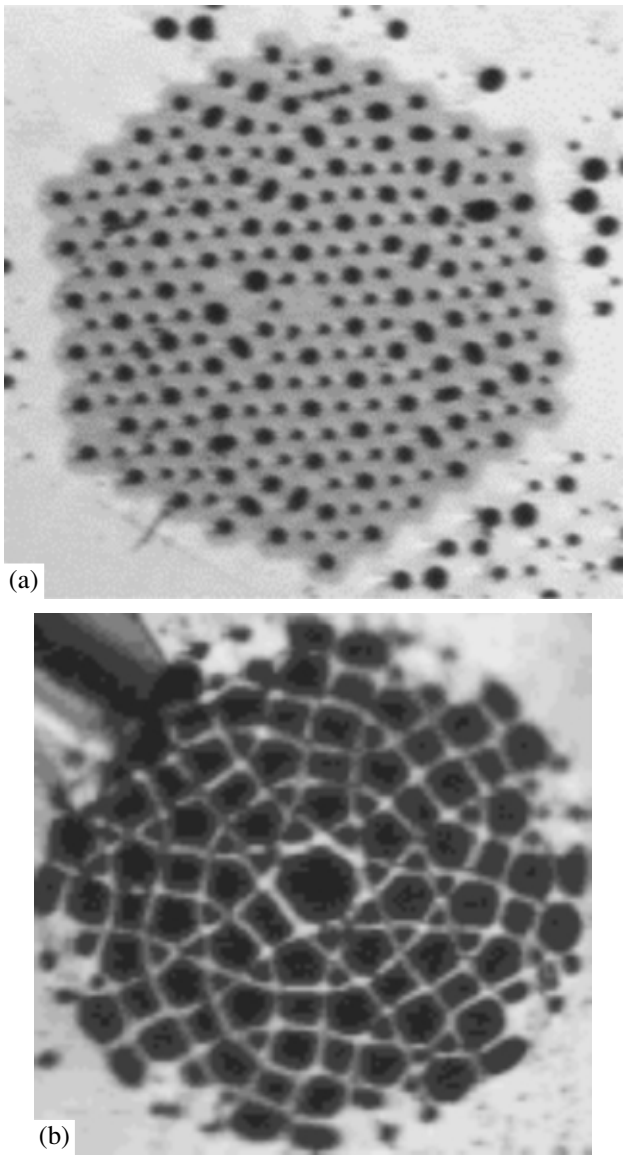

Fig. 1. Cross-sectional microscope images of microstructure fibers: (a) a microstructure fiber with a photonic-crystal cladding, where the air holes are arranged in a spatially periodic way, and (b) a photonic-molecule cobweb-microstructure-integrated bundle of fibers with a radius of each fiber in the bundle equal to 2 μm and the distance between the neighboring fibers of 7.4 μm.

ing hole, serving as a fiber core (Fig. 1a). Microstructure fibers of the second type have a core with the cross section in the form of a cyclic photonic molecule (Fig. 1b). Air holes arranged in a two-dimensionally periodic structure in the cladding of this fiber and a larger hole at the center of the fiber form a cyclic-molecule-like structure, consisting of an array of small-diameter glass channels linked by narrow bridges, around the central hole (Figs. 1b, 2) [22, 23]. Such a photonic-molecule (PM) microstructure-integrated bundle of fibers can guide the light through total internal reflection, providing a very high light confinement

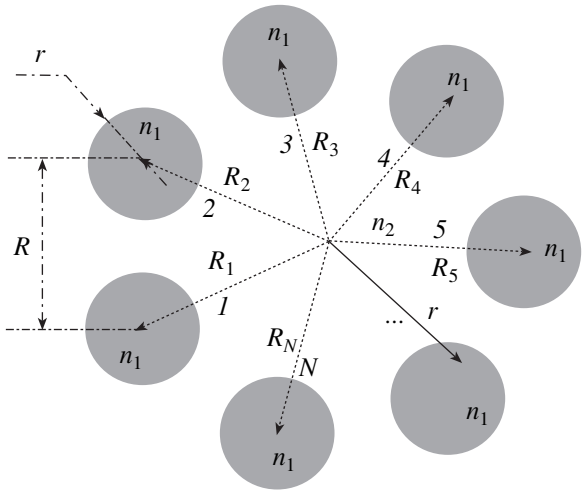

Fig. 2. A photonic-molecule model for an optical fiber where the light is guided along a set of N cores with the refractive index n_1 surrounded by a material with the refractive index n_2 and linked by narrow bridges with the distance between the neighboring cores equal to R.

degree due to the large refractive index step. We will show that fibers of this type offer new solutions to the key problem of nonlinear waveguide optics of very short light pulses, opening the ways to engineer waveguide dispersion and to change the regimes of nonlinear-optical interactions by switching between the photonic-molecule modes of a microstructure fiber.

2. SCALAR DISPERSION THEORY OF A TWO-DIMENSIONAL CYCLIC PHOTONIC MOLECULE

The ring system of fibers linked by narrow glass bridges at the center of our MS fiber (Fig. 1b) is reminiscent in its structure of the configuration of atoms linked by chemical bonds in a cyclic polyatomic molecule consisting of identical atoms (a generic diagram of such a molecule is shown in Fig. 2). This photonic-molecule analogy will later prove to be quite rewarding by providing us with an illustrative and physically clear model of dispersion properties and mode structure of the considered rather complicated optical fiber. Physical and mathematical aspects of the analogy between a bundle of coupled microstructure-integrated fibers and a polyatomic molecule should be emphasized. Physically, the action of a refractive-index step in the cross section of an MS fiber (the plane of Fig. 2) on a light field is similar to the influence of a potential distributed in space on an electron wave function in a molecular system. Mathematically, this analogy stems from the similarity of coupled-theory equations for electromagnetic radiation in an array of coupled fibers [24] to perturbation-theory equations for the electron wave function in a polyatomic molecule. Earlier, an elegant model of a diatomic PM has been used to describe the

modes of coupled semiconductor [25] and dye-doped polymer [26] microcavities.

Our photonic-molecule microstructure-integrated bundle of fibers can guide the light through total internal reflection, providing a very high light confinement degree due to the large refractive index step on the glass–air interface (Fig. 3). Due to this property, MS fibers of the considered type offer much promise for enhancing nonlinear-optical interactions and reducing the lasing threshold in micro- and nanostructured laser materials.

In our analysis of mode properties of radiation guided in a PM fiber, we will neglect polarization effects (the vector theory of dispersion of a two-dimensional cyclic photonic molecule will be published elsewhere) and employ a scalar-wave-equation approximation [24] to consider a set of N cyclically coupled identical channels with the refractive index n_1 surrounded by a material with the refractive index n_2 (Fig. 2). Since the strongest mode coupling is achieved for waveguide modes with equal propagation constants in a photonic-molecule fiber with identical cores, we will neglect also the coupling of modes with different propagation constants. The modes of the PM fiber can be then represented as superpositions of modes of isolated fibers:

$$\Psi(\mathbf{r}) = \sum_n A_n f(\mathbf{r} - \mathbf{R}_n), \quad (1)$$

where $\mathbf{r}$ is the radius vector in the plane of fiber cross section (the plane of Fig. 2), $\mathbf{R}_n$ are the coordinates of the center of the nth fiber in the same plane, and A_n and $f(\mathbf{r} - \mathbf{R}_n)$ are the amplitude and the transverse distribution of the field in the guided mode in the nth fiber. Since only the neighboring fibers are coupled to each other in our photonic-molecule bundle, the coupled-mode equations for the field amplitudes can be written as [24]

$$\frac{dA_n}{dz} - i\beta A_n - i\alpha(A_{L(n)} + A_{R(n)}) = 0, \quad (2)$$

where β is the propagation constant for the relevant guided mode of an isolated fiber,

$$\alpha = \frac{\omega^2}{2\beta c^2} \frac{\int \Delta\varepsilon(\mathbf{r}) f(\mathbf{r} - \mathbf{R}_{n'}) f^*(\mathbf{r} - \mathbf{R}_n) d\mathbf{r}}{\int |f(\mathbf{r} - \mathbf{R}_n)|^2 d\mathbf{r}} \quad (3)$$

is the coefficient characterizing mode coupling for the nth and $(n \pm 1)$th fibers in the considered structure (ω is the radiation frequency and $\Delta\varepsilon(\mathbf{r})$ is the deviation from the unperturbed dielectric constant at a given point with a radius vector $\mathbf{r}$), and

$$L(n) = \begin{cases} n-1, & n > 0 \\ N, & n = 0, \end{cases}$$

$$R(n) = \begin{cases} n+1, & n < N \\ 1, & n = N. \end{cases}$$

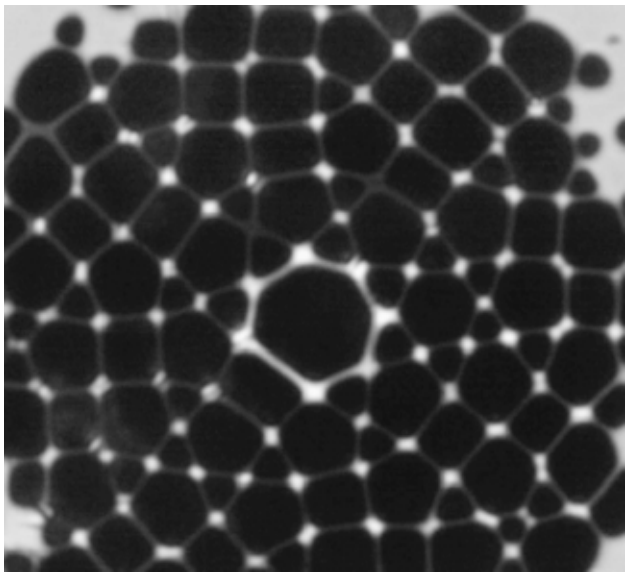

Fig. 3. The spatial distribution of light intensity in the fundamental photonic-molecule mode excited with helium–neon laser radiation in a cobweb microstructure fiber shown in Fig. 1b.

The propagation constants can now be found from the characteristic equation corresponding to the set of equations (2). In the general case of arbitrary N, these propagation constants can be calculated with the use of numerical methods. There are several simple analytical solutions, however, that provide a useful physical insight into the dispersion of the photonic-molecule fiber. In particular, a symmetric field distribution,

$$\Psi_1(\mathbf{r}) = A \sum_n f(\mathbf{r} - \mathbf{R}_n), \quad (4)$$

where A is a constant, is allowed by Eq. (2) for any N. This symmetric mode of our fiber is similar to a symmetric wave function of a polyatomic molecule. The propagation constant for such a symmetric mode is given by

$$B_1 = \beta + 2\alpha. \quad (5)$$

Expression (5) shows that mode coupling in the considered array of fibers results in a renormalization of propagation constants.

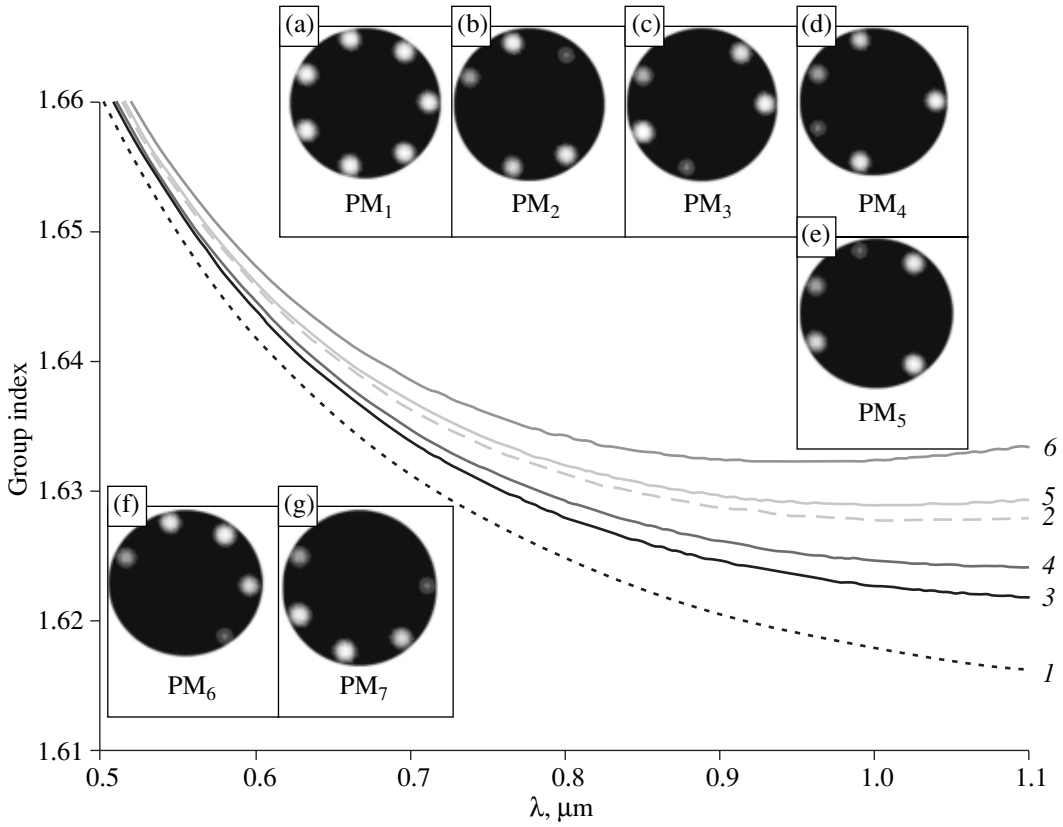

Fig. 4. The group index as a function of radiation wavelength for (*1*) the material of the fiber; (*2*) a single isolated fiber from the considered photonic-molecule structure (or an array of identical fibers completely isolated from one another); and (*3*) PM_1, (*4*) PM_2 and PM_3, (*5*) PM_4 and PM_5, and (*6*) PM_6 and PM_7 modes of a seven-core photonic-molecule fiber ($N = 7$). The radius of a single elementary fiber in the photonic-molecule fiber structure is 2 μm, the distance between the neighboring fibers in the photonic-molecule structure is 7.4 μm. The insets show light intensity distributions in (a) PM_1, (b) PM_2, (c) PM_3, (d) PM_4, (e) PM_5, (f) PM_6, and (g) PM_7 modes of a seven-core cobweb microstructure fiber.

An antisymmetric solution

$$\Psi_N(\mathbf{r}) = A\sum_n (-1)^n f(\mathbf{r}-\mathbf{R}_n) \qquad (6)$$

is also allowed by Eq. (2) for even N. This antisymmetric mode also has an obvious analogy in quantum chemistry. The propagation constant is then renormalized in accordance with

$$B_N = \beta - 2\alpha. \qquad (7)$$

We identify the fundamental mode of our PM fiber as the mode with the largest propagation constant. The highest value of the propagation constant in the case under consideration is achieved for the symmetric mode. In terms of the point-group symmetry, this mode possesses a full rotational symmetry of an idealized PM fiber with a perfect rotational symmetry (cf. Figs. 1b and 2). We introduce the mode index l to enumerate PM-fiber modes, which will be denoted as PM_l modes, starting with $l = 1$, which corresponds to the fundamental PM mode.

Numerical simulations were performed for a PM fiber structure that modeled the MS fiber employed in our experiments and that consisted of seven identical glass cores with a radius $a = 2$ μm. The refractive index of the cladding was set equal to the refractive index of atmospheric-pressure air ($n_2 = 1$). The distance R between the neighboring cores was 7.4 μm. To estimate the coupling coefficient appearing in Eq. (2), we employed the expression for the coupling coefficient, $\alpha = C\lambda$, where λ is the wavelength, from the model of two coupled identical planar waveguides [24]. For characteristic geometric sizes of our structure, this model allows the parameter C to be estimated as 0.016 μm^{-1}. Only lowest order modes of isolated fibers were included in our calculations. The inclusion of higher order modes will, of course, change dispersion branches of a PM fiber and make the analysis much more complicated. The model that includes only fundamental modes of each elementary fiber, on the other hand, allows the general physical features of dispersion of a PM fiber to be understood without reproducing the fiber dispersion in all the details.

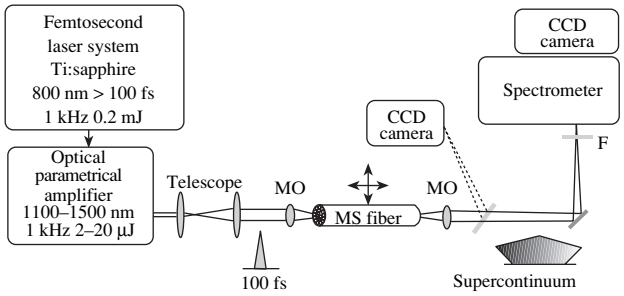

Fig. 5. Frequency-tunable femtosecond laser system based on an optical parametric amplifier: MO, microobjectives; F, system of optical filters.

Figure 4 displays the group index as a function of radiation wavelength for the material of the fiber (curve *1*), a single isolated fiber from the considered photonic-molecule structure (curve *2*), and PM_1–PM_7 modes of the considered seven-core MS fiber (curves *3*–*6*). The transverse light intensity distributions corresponding to these modes are shown in the insets *a*–*g* in Fig. 4. The lowest value of the group index, as can be seen from the results presented in Fig. 4, is achieved for the PM_1 fundamental mode. Higher order PM modes are characterized by lower group velocities, implying that nonlinear-optical processes should be enhanced for these modes.

3. EXPERIMENTAL

Microstructure fibers were fabricated with the use of the technique that now becomes standard [1, 27] and that involves stacking capillaries into a preform and then pulling this preform at elevated temperatures. A preform with a capillary of a larger inner diameter at the center was used to fabricate MS fibers studied in this paper, resulting in a special configuration of holes shown in Fig. 1b.

Femtosecond pulses were produced in our experiments by a laser system [28] consisting of a Ti:sapphire master oscillator, a multipass amplifier, and an optical parametric amplifier (OPA) based on a BBO crystal (Fig. 5). This laser system generated laser pulses with a wavelength tunable from 1.1 to 1.5 μm. The best performance of the OPA system was achieved at the wavelength of 1.25 μm, where light pulses with a duration of approximately 80 fs were produced.

Laser radiation was coupled into an MS fiber sample placed on a three-coordinate translation stage with the use of a microobjective. The efficiency of waveguide mode excitation in the MS fiber was monitored by imaging the light field distribution at the output end of the fiber onto a CCD camera (Fig. 5) and by measuring the total energy of radiation coming out of the fiber.

The model of optical properties of photonic-molecule modes in an MS fiber described in Section 2 of this

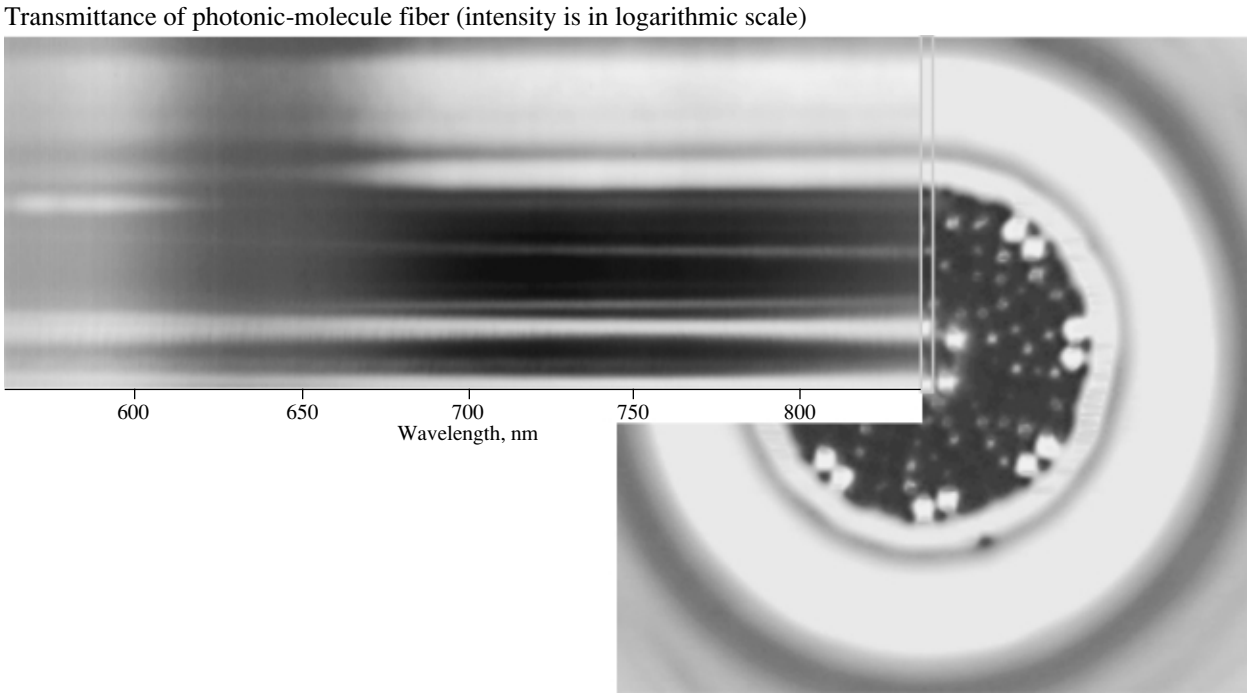

Fig. 6. Results of space- and frequency-resolved measurements of optical losses in photonic-molecule modes of a cobweb microstructure fiber. The intensity is shown by levels of gray on a logarithmic scale. The spectrally resolved spatial distribution of radiation intensity at the output of the fiber is shown on the left.

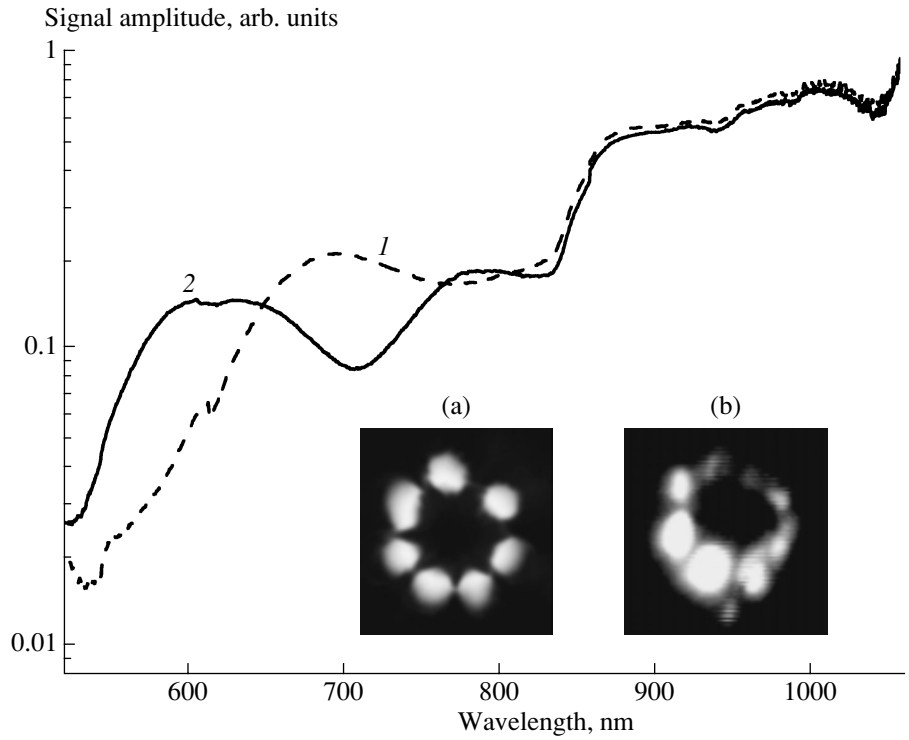

Fig. 7. The spectra of supercontinuum generated in the (*1*) PM_1 and (*2*) PM_6/PM_7 modes of a photonic-molecule fiber with a length of 4 cm. OPA radiation pulses with the wavelength of 1.30 μm and the energy of 100 nJ are coupled into the fiber. The initial duration of light pulses is 80 fs. The radius of a single fiber in the PM fiber structure is 2 μm, and the distance between the neighboring fibers in the PM structure is 7.4 μm. The insets show white-light images of PM fibers produced with the use of supercontinuum generated in (a) the PM_1 and (b) PM_6/PM_7 modes of such a fiber by 80-fs 100-nJ pulses of 1.3-μm OPA radiation.

paper does not include guiding losses inherent in such modes. Such losses is an important factor having a considerable influence on the efficiency of nonlinear-optical processes in such guided modes and limiting in many cases the fiber length. To estimate the magnitude of optical losses, we performed direct space- and frequency-resolved measurements of attenuation of radiation guided in photonic-molecule modes of our MS fiber. The results of these measurements are presented in Fig. 6. In view of these results, we employed fiber samples with a typical length of several centimeters for our experiments in order to reduce the influence of radiation losses.

4. SUPERCONTINUUM GENERATION IN MICROSTRUCTURE FIBERS: PHOTONIC MOLECULES VERSUS THE PHOTONIC-CRYSTAL GEOMETRY

Varying the focusing geometry and shifting the fiber end with respect to the light beam coupled into the fiber, we were able to excite, in fact, all the PM_l fiber modes with $l = 1, 2, \ldots, 7$. We observed efficient spectral broadening of femtosecond OPA pulses and supercontinuum generation for all these modes. The efficiency of supercontinuum generation in higher order PM modes was noticeably higher than the efficiency of white-light generation in the fundamental PM mode. Figure 7 presents the spectra of supercontinuum emission produced in PM_1 and PM_6/PM_7 modes in a 4-cm PM-fiber sample (the spatial distributions of radiation intensity at the output of the fiber are shown in the insets in Fig. 7). Comparison of curves *1* and *2* in Fig. 7 shows that the supercontinuum emission generated in the PM_6 and PM_7 modes had a noticeably broader bandwidth than the supercontinuum generated in the fundamental mode. The spectrum of the supercontinuum generated by 80-fs pulses of 1.3-μm OPA radiation in the PM_6/PM_7 mode of our fiber reached approximately one octave starting with the laser pulse energy of about 100 nJ.

The efficiency of supercontinuum generation in photonic-molecule modes of microstructure fibers is typically lower than the efficiency of supercontinuum generation in standard single-core photonic-crystal fibers (cf. Figs. 7 and 8). This is mainly due to the larger total effective mode area in the case of PM fibers (cf. Figs. 1a and 1b). However, due to their design, photonic-molecule fibers offer several important options, which seem to advantageously supplement vast opportunities provided by photonic-crystal fibers. In particular, additional dispersion tunability can be achieved in

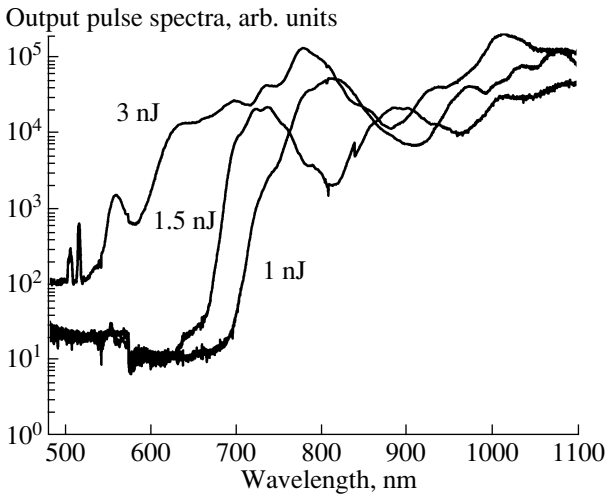

Fig. 8. The spectra of laser pulses coming out of photonic-crystal fibers with an air-filling fraction of 16%, the length of 4 cm, and the core radius equal to 1.5 μm. OPA pulses with a duration of about 80 fs and the wavelength of 1.25 μm are coupled into the fiber. The energies of pulses coupled into the fiber are specified near the curves.

the case of PM fibers by varying the initial conditions at the input end of the fiber, resulting in the excitation of different PM fiber modes. A promising direction for further studies would be to explore the possibility of coherent control of nonlinear-optical cross-action processes in the fibers of a PM waveguiding structure by using pulses with different temporal and spatial profiles, frequencies, and initial chirps. It would be of interest also to search for new ways to phase-match nonlinear-optical interactions in such fibers, as well as to examine the potential of PM fibers for pulse compression through self- and cross-phase modulation and supercontinuum generation. The geometry of PM fibers is also advantageous for evanescent-field sensing and broadband evanescent-field spectroscopy of gases or liquids using supercontinuum generation, as well as for the laser guiding of atoms.

5. CONCLUSION

Thus, we have demonstrated that the modes guided in a ring system of microstructure-integrated fibers have much in common with electron wave functions in a two-dimensional polyatomic cyclic molecule. The photonic-molecule model provides an illustrative qualitative description of dispersion properties and the mode structure of electromagnetic field in microstructure fibers of the considered type. A high degree of light confinement in waveguide modes of such a photonic-molecule fiber enhances nonlinear-optical processes, permitting an octave spectral broadening to be achieved for low-energy femtosecond laser pulses.

ACKNOWLEDGMENTS

This study was supported in part by the President of Russian Federation Grant no. 00-15-99304, the Russian Foundation for Basic Research project no. 00-02-17567, Volkswagen Foundation (project I/76 869), CRDF Award no. RP2-2266, and federal science and technology programs of Russian Federation.

REFERENCES

1. Knight, J.C., Birks, T.A., Russell, P.St.J., and Atkin, D.M., 1996, *Opt. Lett.*, **21**, 1547; Knight, J.C., Broeng, J., Birks, T.A., and Russell, P.St.J., 1998, *Science*, **282**, 1476.
2. Bennet, P.J., Monro, T.M., and Richardson, D.J., 1999, *Opt. Lett.*, **24**, 1203.
3. Zheltikov, A.M., 2000, *Usp. Fiz. Nauk*, **170**, 1203.
4. 2001, *Opt. Express*, **9**, special issue.
5. Broderick, N.G.R., Monro, T.M., Bennett, P.J., and Richardson, D.J., 1999, *Opt. Lett.*, **24**, 1395.
6. Fedotov, A.B., Zheltikov, A.M., Tarasevitch, A.P., and von der Linde, D., 2001, *Appl. Phys. B*, **73**, 181; Zheltikov, A.M., Alfimov, M.V., Fedotov, A.B., Ivanov, A.A., Syrchin, M.S., Tarasevich, A.P., and von der Linde, D., 2001, *Zh. Eksp. Teor. Fiz.*, **120**, 570.
7. Ranka, J.K., Windeler, R.S., and Stentz, A.J., 2000, *Opt. Lett.*, **25**, 25.
8. Diddams, S.A., Jones, D.J., Jun Ye, Cundiff, S.T., Hall, J.L., Ranka, J.K., Windeler, R.S., Holzwarth, R., Udem, T., and Hänsch, T.W., 2000, *Phys. Rev. Lett.*, **84**, 5102; Jones, D.J., Diddams, S.A., Ranka, J.K., Stentz, A., Windeler, R.S., Hall, J.L., and Cundi, S.T., 2000, *Science*, **288**, 635.
9. Holzwarth, R., Udem, T., Hänsch, T.W., Knight, J.C., Wadsworth, W.J., and Russell, P.St.J., 2000, *Phys. Rev. Lett.*, **85**, 2264.
10. Bagayev, S.N., Dmitriyev, A.K., Chepurov, S.V., Dychkov, A.S., Klementyev, V.M., Kolker, D.B., Kuznetsov, S.A., Matyugin, Yu.A., Okhapkin, M.V., Pivtsov, V.S., Skvortsov, M.N., Zakharyash, V.F., Birks, T.A., Wadsworth, W.J., Russell, P.St.J., and Zheltikov, A.M., 2001, *Laser Phys.*, **11**, 1270.
11. Ranka, J.K., Windeler, R.S., and Stentz, A.J., 2000, *Opt. Lett.*, **25**, 796.
12. Fedotov, A.B., Yakovlev, V.V., and Zheltikov, A.M., 2002, *Laser Phys.*, **12**, no. 2 (in press); Naumov, A.N. and Zheltikov, A.M., 2002, *Opt. Express*, **2**, 122.
13. Husakou, A.V. and Herrmann, J., 2001, *Phys. Rev. Lett.*, **87**, 203901-4.
14. Cregan, R.F., Mangan, B.J., Knight, J.C., Birks, T.A., Russell, P.St.J., Roberts, P.J., and Allan, D.C., 1999, *Science*, **285**, 1537.
15. Naumov, A.N. and Zheltikov, A.M., *Quantum Electron.* (in press).
16. Naumov, A.N. and Zheltikov, A.M., in preparation.
17. Ivanov, A.A., Alfimov, M.V., Fedotov, A.B., Podshivalov, A.A., Chorvat, D., Chorvat, D., Jr., and Zheltikov, A.M., 2001, *Laser Phys.*, **11**, 158.

18. Hartl, I., Li, X.D., Chudoba, C., Rhanta, R.K., Ko, T.H., Fujimoto, J.G., Ranka, J.K., and Windeler, R.S., 2001, *Opt. Lett.*, **26**, 608.
19. Kurnit, N.A., Abella, I.D., and Hartmann, S.R., 1964, *Phys. Rev. Lett.*, **13**, 567.
20. Ortigosa-Blanch, A., Knight, J.C., Wadsworth, W.J., Arriaga, J., Mangan, B.J., Birks, T.A., and Russell, P.St.J., 2000, *Opt. Lett.*, **25**, 1325.
21. Steel, M.J., White, T.P., Martijn de Sterke, C., McPhedran, R.C., and Botten, L.C., 2001, *Opt. Lett.*, **26**, 488.
22. Fedotov, A.B., Naumov, A.N., Konorov, S.O., Beloglazov, V.I., Mel'nikov, L.A., Skibina, N.B., Sidorov-Biryukov, D.A., Shcherbakov, A.V., and Zheltikov, A.M., *Laser Phys.* (in press).
23. Fedotov, A.B., Bugar, I., Naumov, A.N., Chorvat, D., Jr., Sidorov-Biryukov, D.A., Chorvat, D., and Zheltikov, A.M., *Pis'ma Zh. Eksp. Teor. Fiz.* (in press).
24. Yariv, A. and Yeh, P., 1984, *Optical Waves in Crystals: Propagation and Control of Laser Radiation* (New York: Wiley).
25. Bayer, M., Gutbrod, T., Reithmaier, J.P., Forchel, A., Reinecke, T.L., Knipp, P.A., Dremin, A.A., and Kulakovskii, V.D., 1998, *Phys. Rev. Lett.*, **81**, 2582.
26. Mukaiyama, T., Takeda, K., Miyazaki, H., Jimba, Y., and Kuwata-Gonokami, M., 1999, *Phys. Rev. Lett.*, **82**, 4623.
27. Fedotov, A.B., Zheltikov, A.M., Mel'nikov, L.A., Tarasevitch, A.P., and von der Linde, D., 2000, *JETP Lett.*, **71**, 281.
28. Fedotov, A.B., Naumov, A.N., Bugar, I., Chorvat, D., Jr., Sidorov-Biryukov, D.A., Chorvat, D., and Zheltikov, A.M., 2002, *IEEE J. Selected Topics Quantum Electron.* (in press).